

11
18-51
009185

A Normal Incidence X-ray Telescope (NIXT) Sounding Rocket Payload

NASA Grant NAG5-626

Seminnual Reports

For the Periods 1 July 1992 - 31 December 1992, 1 January 1993 - 30 June 1993,
1 July 1993 - 31 December 1993, 1 January 1994 - 30 June 1994,
1 July 1994 - 31 December 1994, 1 January 1995 - 31 July 1995,

Annual Reports

1 August 1995 - 31 July 1996

Principal Investigator
Dr. Leon Golub

September 1996

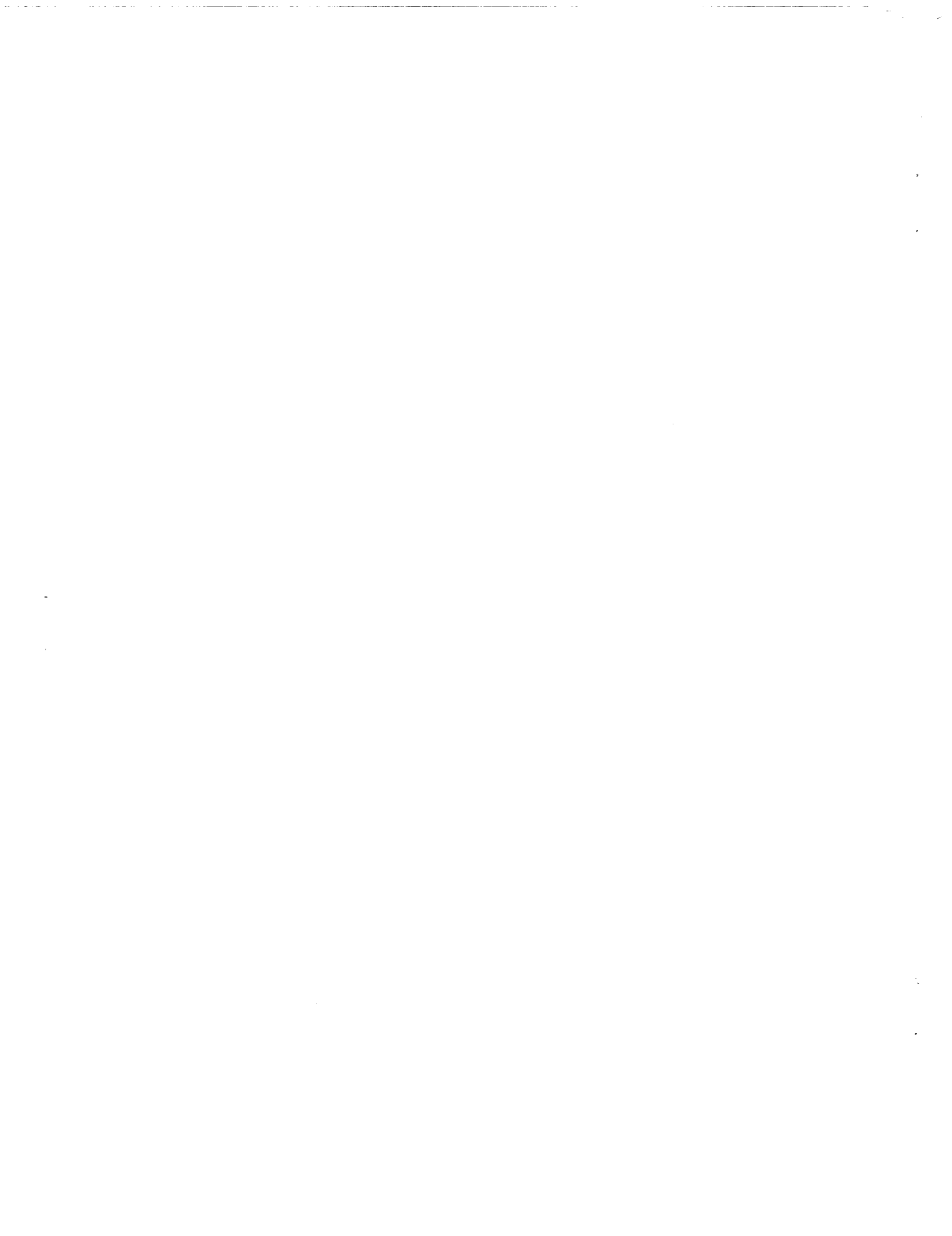
Prepared for:

National Aeronautics and Space Administration
GSFC/Wallops Flight Facility
Wallops Island, Virginia 23337

Smithsonian Institution
Astrophysical Observatory
Cambridge, Massachusetts 02138

The Smithsonian Astrophysical Observatory
is a member of the
Harvard-Smithsonian Center for Astrophysics

The NASA Technical Officer for this grant is Dr. Ray H. Pless, Code 820.0, NASA/GSFC, Wallops Flight Facility, Wallops Island, Virginia 23337.





REVIEW ROUTING SLIP
PROGRESS REPORT

TITLE: NIXT SOUNDING ROCKET PAYLOAD

DIVISION: High Energy Astrophysics Division
Fund No. 16646040 Grant No. NAG5-626

| | INITIALS | DATE | COMMENTS |
|--|----------|---------|----------|
| 1. COORDINATOR Richard F. Vannelli | RV | 9/17 | |
| 2. PRINCIPAL INVESTIGATOR L. Golub | LG | 9/17 | |
| 3. ASSOCIATE DIRECTOR Stephen S. Murray | SM | 9/15 | |
| 4. CONTRACTS' DEPARTMENT George D. Dick | GD | 9/18/96 | |

SEP 24 1996

9/23/96

Progress Report

I. Work Completed During the Past Year:

During the past year we have completed the changeover from the NIXT program to the new TXI sounding rocket program. The NIXT effort, aimed at evaluating the viability of the remaining portions of the NIXT hardware and design, has been finished and the portions of the NIXT which are viable and flightworthy, such as filters, mirror mounting hardware, electronics and telemetry interface systems, are now part of the new rocket payload.

The backup NIXT multilayer-coated x-ray telescope and its mounting hardware have been completely fabricated and are being stored for possible future use in the TXI rocket. The H-alpha camera design is being utilized in the TXI program for real-time pointing verification and control via telemetry.

Two papers, summarizing scientific results from the NIXT rocket program, have been written and published this year:

1. "The Solar X-ray Corona," by L. Golub, *Astrophysics and Space Science*, **237**, 33 (1996).

This is an invited contribution to a Festschrift in honor of Sir Robert Wilson, representing an introduction to the physics of the solar corona. A major portion of the discussion is a summary of results from the series of NIXT sounding rocket flights.

A copy of this paper is appended to this report as Appendix 1.

2. "Difficulties in Observing Coronal Structure," Keynote Paper, Proceedings STEPWG1 Workshop on *Measurements and Analyses of the Solar 3D Magnetic Field, Solar Physics*, (in press, 1996).

There has developed in recent years a substantial body of evidence to indicate that the temperature and density structure of the corona are far more complicated than had previously been thought. We review some of the evidence and discuss some specific examples: observations of a limb flare, showing that the cool H-alpha material is *cospatial* with the hot x-ray emitting material; simultaneous NIXT and Yohkoh SXT observations of an active region, showing that loops seen in one instrument are not seen in the other, and that the effect works

in *both* directions.

Comparisons of extrapolated magnetic field measurements to the observed coronal structure, indicating that neither potential nor constant-alpha force-free fits are adequate. We conclude with a description of two new instruments, the TRACE and the TXI, which will help to resolve some of these difficulties.

A copy of this paper is appended to this report as Appendix 2.

II. Future plans: None.

THE SOLAR X-RAY CORONA

L. GOLUB

*Smithsonian Astrophysical Observatory
60 Garden St., Cambridge MA.*

Abstract. The solar corona, and the coronae of solar-type stars, consist of a low-density magnetized plasma at temperatures exceeding 10^6 K. The primary coronal emission is therefore in the UV and soft x-ray range. The observed close connection between solar magnetic fields and the physical parameters of the corona implies a fundamental role for the magnetic field in coronal structuring and dynamics. Variability of the corona occurs on all temporal and spatial scales – at one extreme, as the result of plasma instabilities, and at the other extreme driven by the global magnetic flux emergence patterns of the solar cycle.

1. Introduction

The corona is a portion of the Sun's outer atmosphere beginning slightly above the visible surface and extending many solar radii out. A precise definition of the term "corona" is to some extent dependent on one's theoretical bias, and one may choose to think in terms of a modified plane-parallel model, or in terms of a composite, multi-component model made up of relatively isolated individual structures.

In either case, the most important physical fact about the corona is that it reaches very high temperatures, more than 10^6 K. Moreover, this temperature increase is found to occur over very short distances, with the rise from $< 10^4$ K to $> 10^6$ K occurring within less than a thousandth of the solar radius. If we pick a temperature well above that of the photosphere, such as 10^5 K, then we may define any portion of the atmosphere above this temperature as *corona*. Because the rise in temperature is so dramatically steep, this choice is adequate for many purposes, since a large change in this cutoff value will correspond to only a very small change in actual physical location.

At visible wavelengths, the corona is extremely faint relative to the disk, having a maximum brightness ratio of $\approx 10^{-6}$, decreasing to $\approx 10^{-9}$ within a single solar diameter away from the visible limb. However, at UV and soft x-ray wavelengths, the situation is reversed. Because of the high temperature of the coronal gas, its primary emission is in the UV and soft x-ray portion of the spectrum. Therefore, an instrument in which the visible light is blocked while the short wavelengths are transmitted permits viewing of the coronal emission on the disk and out to several solar radii above the limb.

Figure 1 shows a superposition of both on-disk and limb observations. It was obtained during a total solar eclipse in 1991, using ground-based data from the CFH-T in Hawaii and x-ray data from the NIXT sounding

rocket (Golub *et al.* 1990). The ground-based eclipse permitted the white-light photo of the outer corona to be obtained, while the *uneclipsed* sun was viewed at the same time from above White Sands, New Mexico, where the eclipse had not yet started. The combination of the two observations shows that the streamer structures originate at the solar surface, typically in the brighter places called "active regions." This type of comparison brings home clearly the point that the corona is three-dimensional, with its roots at or below the solar photosphere and outer extension far into interplanetary space.

Observations of the high-temperature solar emission were first carried out from sounding rockets (Baum *et al.* 1946) and techniques for high resolution x-ray imaging were developed under NASA's Suborbital program (Vaiana, Krieger & Timothy 1973) during the late 60's and early 70's. The high temperature corona emits predominantly in isolated spectral lines which fall in the XUV and soft x-ray spectral regions, and many of the important lines were observed and identified by Sir Robert and co-workers in the 60's (Wilson 1964; Jones, Freeman & Wilson 1968). These studies and technological development efforts led to the first series of high resolution studies with extended temporal coverage, carried out from *Skylab* (*viz.* Orrall 1981); these will be discussed in the next section. Most recently, the *Yohkoh* satellite has significantly advanced the study of coronal activity and variability, using a combination of soft x-ray and hard x-ray imaging to study coronal activity, and a major new solar observatory – the Solar and Heliospheric Observatory (SoHO) – carries a large complement of instruments which are expected to provide a comprehensive view of the sun from its interior out to the solar wind.

The solar-stellar connection

If our sun, which is a typical middle-aged low-mass star, has a corona and is a source of x-ray emission, then it is reasonable to ask whether other stars also have coronae and emit x-rays. Within the past two decades this question has been answered in the affirmative: not only do other stars emit x-rays, but the sun is rather below average in activity level. Stars of nearly all spectral types are found to emit UV and x-rays and to display tracers of activity which are detectable in ground-based observations.

Ground-based observations may be used to determine the level of activity on stars, using methods which range from detection of chromospheric lines (Wilson 1963) to direct detection of magnetic fields (Robinson, Worden & Harvey 1980). Surveys of all spectral types, but especially of solar-type stars, have been carried out, most notably at Mt. Wilson (Vaughan 1980).

The direct detection of material at transition region and coronal temperatures had to await observations from space: the International Ultraviolet



Fig. 1. Composite photo showing the white-light corona seen from the CFH-T in Hawaii at the 11 July 1991 eclipse and the on-disk x-ray corona observed from the NIXT sounding rocket at the same time.

Explorer (IUE) was launched into a quasi-geosynchronous * orbit on 26 January 1978. The satellite provided ultraviolet spectra of astronomical objects ranging from comets and planets to active galactic nuclei and quasars. For stellar studies, the spectra extended the ground-based observations to more highly ionized species, such as Si IV, C IV and N V, thus permitting the extension of ground-based chromospheric studies into what would appear to

* The satellite circulates over Central and South America in a pattern which allows access by ground stations feeding both Europe and North America.

be temperatures more characteristic of the chromosphere-corona transition region.

Early IUE surveys extended our knowledge of high-temperature atmospheres on solar-type stars, and also showed a cutoff in coronal emission for late-type giants and supergiants (Linsky & Haisch, 1979). Detailed analysis of emission from late-type stars shows that in general they are solar-like in their properties, as was shown by data from both the IUE (Linsky 1980) and the *Einstein* Observatory, launched on 13 November 1978.

The *Einstein* Observatory had higher sensitivity to x-rays than previous experiments and it also had the ability to produce high resolution images, which yields a high signal-to-noise ratio. As it turns out, flare stars and RS CVn stars are only a few orders of magnitude brighter than "normal" stars, so that the increase in sensitivity of the *Einstein* observations was more than enough to allow the less active solar-type stars to be seen. A survey published after the first year of observation (Vaiana *et al.*, 1981), showed an "x-ray H-R diagram" nearly indistinguishable from its optical counterpart.

2. Magnetic Fields and X-ray Emission

In seeking to explain the existence of a corona on the sun, the major questions to be answered concern:

- coronal heating: the high temperature seems to compel the need to invoke some non-thermal, i.e., mechanical, source of energy. What is that source and how does it transfer energy to the coronal plasma?
- coronal structure: in addition to the gross correlation between magnetic fields and coronal heating, there is fine structure in the corona. What determines the scale size of the "loops"?
- stability: the overall appearance of the corona is stable on several days' timescale, but instabilities and rapid energy release occur on timescales of minutes and seconds.
- currents: how is energy stored in the corona and what causes its sudden release?

The key to answering these questions seems to be in the close connection between the presence, at and above the photosphere, of strong magnetic fields and the locations of the brightest, hottest regions in the corona. Magnetic flux is seen to emerge from the solar interior, rising and breaking through the surface in the form of bipolar regions. Here 'bipolar' indicates that the magnetic field is re-entrant to the solar surface - field of one polarity emerges and field of the opposite polarity re-enters, usually at a nearby location. The overall appearance is roughly that of the field from a magnetic dipole lying horizontally just below the surface. Corresponding to this magnetic structure, the hot coronal plasma is seen to form loop-shaped structures which appear to trace the magnetic topology.

The life of such a region is divided into two main stages, the emergence of magnetic flux and then the subsequent diffusion of that flux across the solar surface. The x-ray loop structures are seen to emerge and grow in accordance with the evolution of the magnetic field.

These processes are directly observed in the corona by x-ray imaging techniques, and at the photospheric level by magnetic field maps, or magnetograms, which can measure the field strength* directly. The regions of emerged flux are seen in magnetograms as neighboring patches of opposite polarity field. The bottom panel of Fig. 2 shows such a magnetogram.

For large regions containing more than 10^{20} Mx [$1 \text{ Mx} \equiv 1 \text{ gauss-cm}^2$] total flux, the field is seen to emerge, grow in size and then gradually spread out across the solar surface. The calculated timescale for ohmic diffusion of the magnetic field in the photosphere by classical collisional electric resistivity is too slow by many orders of magnitude. It appears necessary to invoke turbulent diffusion, in which the field is moved about by the convective motions at or below the photosphere, in order to account for the rapid spreading of emerged magnetic flux. This process is also, in some theories, closely connected with the heating of the corona, by one of any number of proposed mechanisms whereby the convective motions feed energy into the coronal plasma via the magnetic field (for a recent review, see Narain & Ulmschneider 1990).

Fig. 2 also shows a near-simultaneous coronal x-ray image, taken with the NIXT sounding rocket payload (Golub *et al.* 1990)**. The x-ray image covers temperatures from $1 - 3 \times 10^6$ K, and the hottest, brightest locations coincide with the strongest concentrations of emerged magnetic flux. This can be seen by locating the x-ray bright regions in the top photo and comparing to the black-and-white bipolar magnetic areas in the bottom photo.

Note also that there are extensive regions of weaker magnetic flux in the magnetogram. However, the measured values of magnetic field strength are now known to be deceptively low. The actual photospheric strength of the magnetic field is found to be well over 10^3 G, (Frazier & Stenflo 1972) so that the appearance of weaker average field means that the B is concentrated into small magnetic elements with a low filling factor: the photospheric field is intermittent. In the corona, the field cannot be measured directly, but appears to be space-filling, as expected from the low plasma β . Above the weak-field regions the loop structures are larger and weaker than in active regions; such locations have sometimes been called "quiet corona", but time resolved observations show that it is not at all quiet, as we describe in the next section.

* Either just the line of sight component, or more recently the full vector field.

** The data could not be taken exactly simultaneously because of a total eclipse; note the shadow of the moon entering the x-ray f.o.v. from the west.

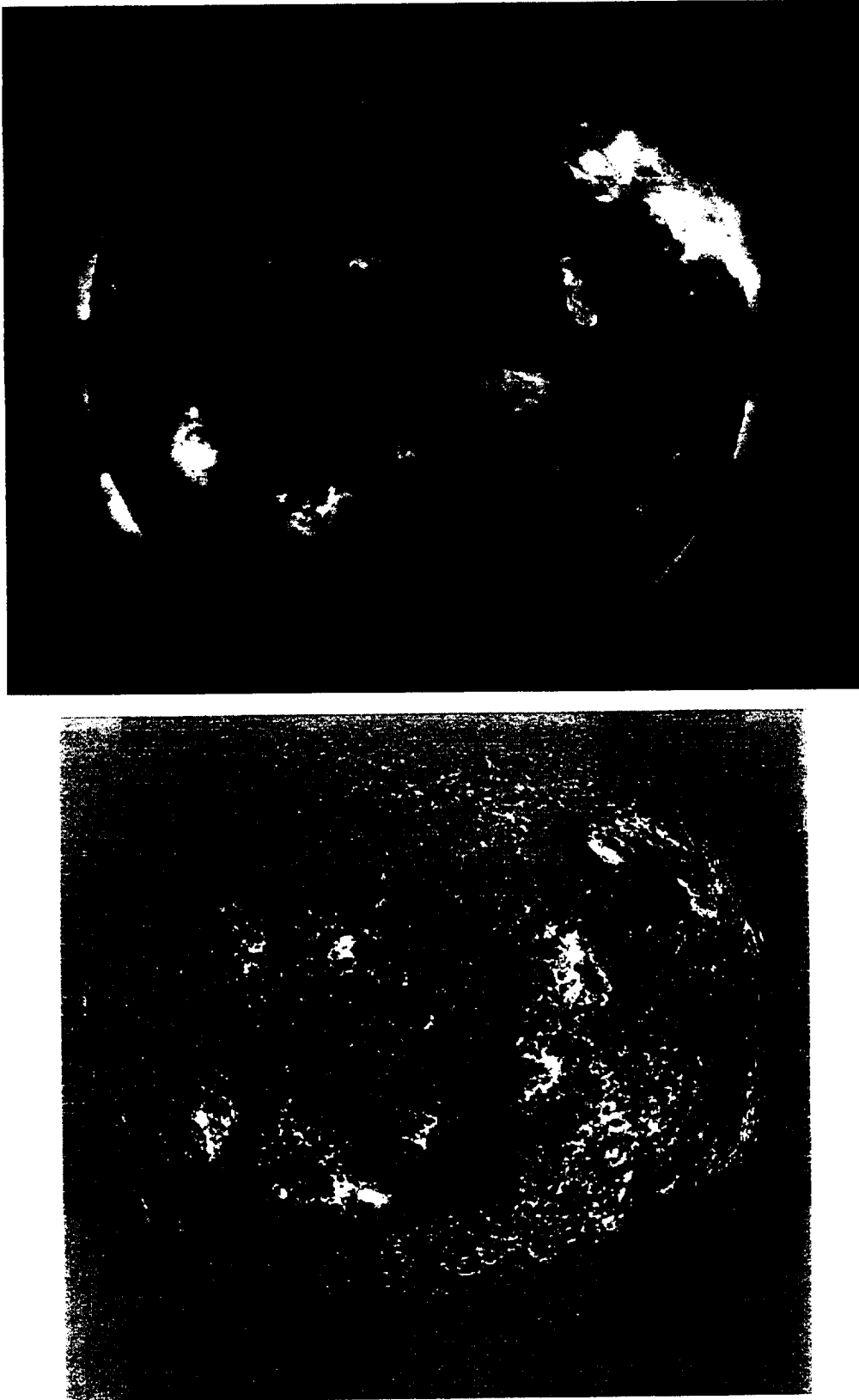


Fig. 2. Near-simultaneous longitudinal magnetic field map (bottom, from NSO/Kitt Peak), and x-ray images of the sun (top, from the NIXT rocket), 11 July 1991.

3. Short-term Variability

X-ray variability.

Prior to *Skylab* it was generally expected that the x-ray corona would show variations on time scales governed by the emergence and diffusion of magnetic flux. Although flares certainly were known, the general view concerning rapid events was that "Coronal events are rare." (Dunn, 1971). This view was completely reversed by the *Skylab* data, leading to the realization that all parts of the corona are varying on nearly every possible timescale (Vaiana & Rosner 1978) and that future instruments should be designed with the capability to obtain both high spatial and temporal resolution coronal imaging (Golub 1991).

An example of the dynamic changes seen in active regions is shown in Fig. 3. The four panels cover about 1-1/2 days and show the changes in the corona induced by the emergence of new magnetic flux near a pre-existing region. The older region is seen to consist of closed (re-entrant) loops and follows the magnetic field in being spread-out and fairly diffuse. To the west (right in this image) a newly emerging region is compact and very bright, with correspondingly strong emerging magnetic field. The dynamic and highly variable x-ray emission in the newly emerging region is evident, as is also the flare-like activity associated with the formation of interconnecting loops between the two regions. The complexity of the coronal structures, i.e. of the magnetized plasma loops, is also quite evident.

Transient loop brightenings.

A study carried out by Sheeley & Golub (1979) using *Skylab* data from the NRL S-082 and AS&E S-054 instruments provided one of the only studies of coronal variability at high spatial and temporal resolution. The study consisted of a set of nested exposures with time resolution down to two minutes at the center of the set, and focussed on two x-ray bright points (XBPs). These are defined as small, short-lived, magnetically bipolar regions of enhanced x-ray emission in the low corona (Golub *et al.* 1974). Active regions (ARs) were also seen in the data, but were excluded from the study because the large number of loops in the ARs made tracking of individual structures difficult.

The XBPs were seen to consist of a small number of loops, the number varying from two to six from one observation to another. Individual loops were seen to brighten and fade rapidly on timescales of about six minutes, which corresponds to the timescale for cooling by radiation and conduction in a plasma with the observed temperature and density. At any given moment, the "bright point" is seen to consist of several "independently-evolving miniature loops". This study concluded that the coronal structures

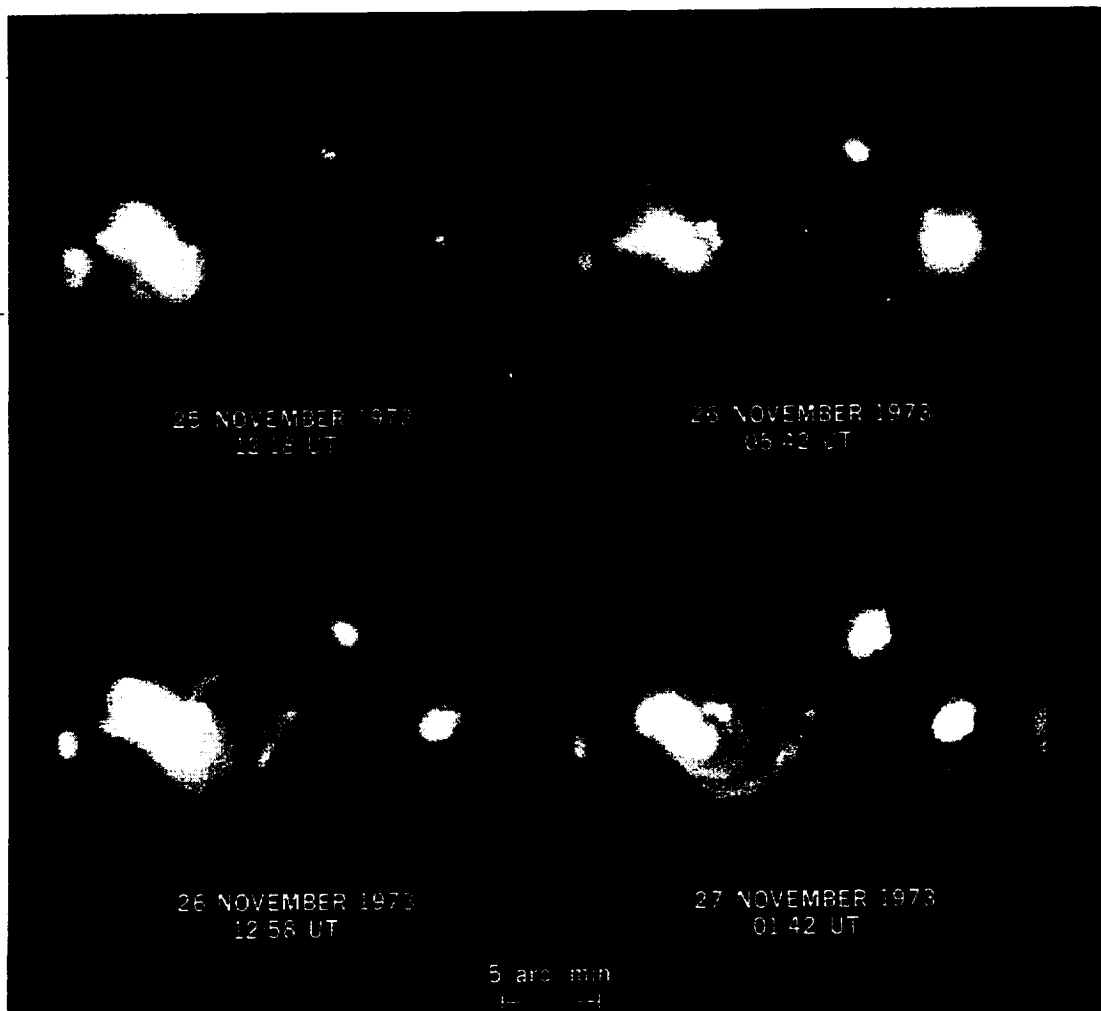


Fig. 3. The rapid reorganization of coronal loop structures in response to newly emerging magnetic flux.

are brightening and fading as fast as they can, and that the observed variability is consistent with an intermittent delta-function energy input, followed by energy redistribution by conduction and radiative losses without significant additional energy input.

The Yohkoh soft x-ray telescope (SXT) has provided the clearest images to date of the extremely dynamic and variable nature of the solar corona. While originally designed primarily as a flare mission, this satellite has proven to be extremely useful for studying the activity of the corona on spatial scales consistent with the resolution (2.5 arcsec pixels) and on temporal scales from seconds to months, and even years.

One of the finest examples of this variability are the so-called "transient brightenings" seen in active regions (Shimizu *et al.* 1992). Some (but not all) active regions are particularly dynamic in showing repeated, small flare-

like brightenings, which are clearly seen to take place in closed magnetic structures, i.e., in “loops”. An example of this phenomenon is shown in Fig. 4, from Shimizu *et al.* (1992).

The brightenings have a power-law spectrum of energy, from 10^{29} erg down to the instrumental threshold at $\approx 10^{25}$ erg, with a slope $\alpha = 1.7$. Thus, the larger-events blend into the distribution of events which one would normally call “flares”, but the slope is not consistent with the suggestion that these brightenings make a significant contribution to the heating of active region coronae (Shimizu 1994).

Flares in x-rays.

Solar flares emit high levels of radiation at nearly all wavelengths, from the radio to x-rays and even gamma rays. Flares and the large-scale magnetic rearrangements in the corona associated with flares, eject relativistic electrons, protons, heavy ions and perhaps neutrinos. They produce microwave radio bursts with timescales of milliseconds and long wavelength radio noise storms lasting days. Coronal soft x-ray emission may increase temporarily by a factor of 1000 in a flare, and enhancements may last several minutes up to tens of hours. At the earth, upper atmospheric disturbances, auroral displays, ground-level particle events and a host of related phenomena are produced.

The definition of a flare is somewhat controversial. An often-used classification defines a flare as ‘a rapid temporary heating of a restricted part of the solar corona and chromosphere.’ However, ‘rapid’ might mean a few seconds or it might mean several hours. ‘Restricted’ may mean a volume so small that it is below our ability to resolve, or it may mean a volume nearly as large as the sun itself. If we ask, how much heating must occur for an event to be called a flare, the possible answers cover a range of six to nine orders of magnitude.

Of course, some things are considered nearly certain. There is nearly universal agreement that magnetic fields play a crucial role in controlling solar activity in general, and flares in particular. We cannot do justice to the extensive range of ideas in the literature on this subject; for details of present flare theory the reader is referred to Tandberg-Hanssen & Emslie (1988) and to the article by Priest in this volume.

As an indication of the possible upper end of the flare size scale in the solar corona, Fig. 5 shows the coronal brightening associated with a large filament eruption. This event evolves to a size greater than a solar radius in extent, and such events often are responsible for major readjustments of the large-scale coronal structure. The timescale of this event is long, taking nearly an hour to brighten and several hours to fade away. The latter timescale typically does not agree with the somewhat shorter times calculated for radiative and conductive cooling, so that continued energy input

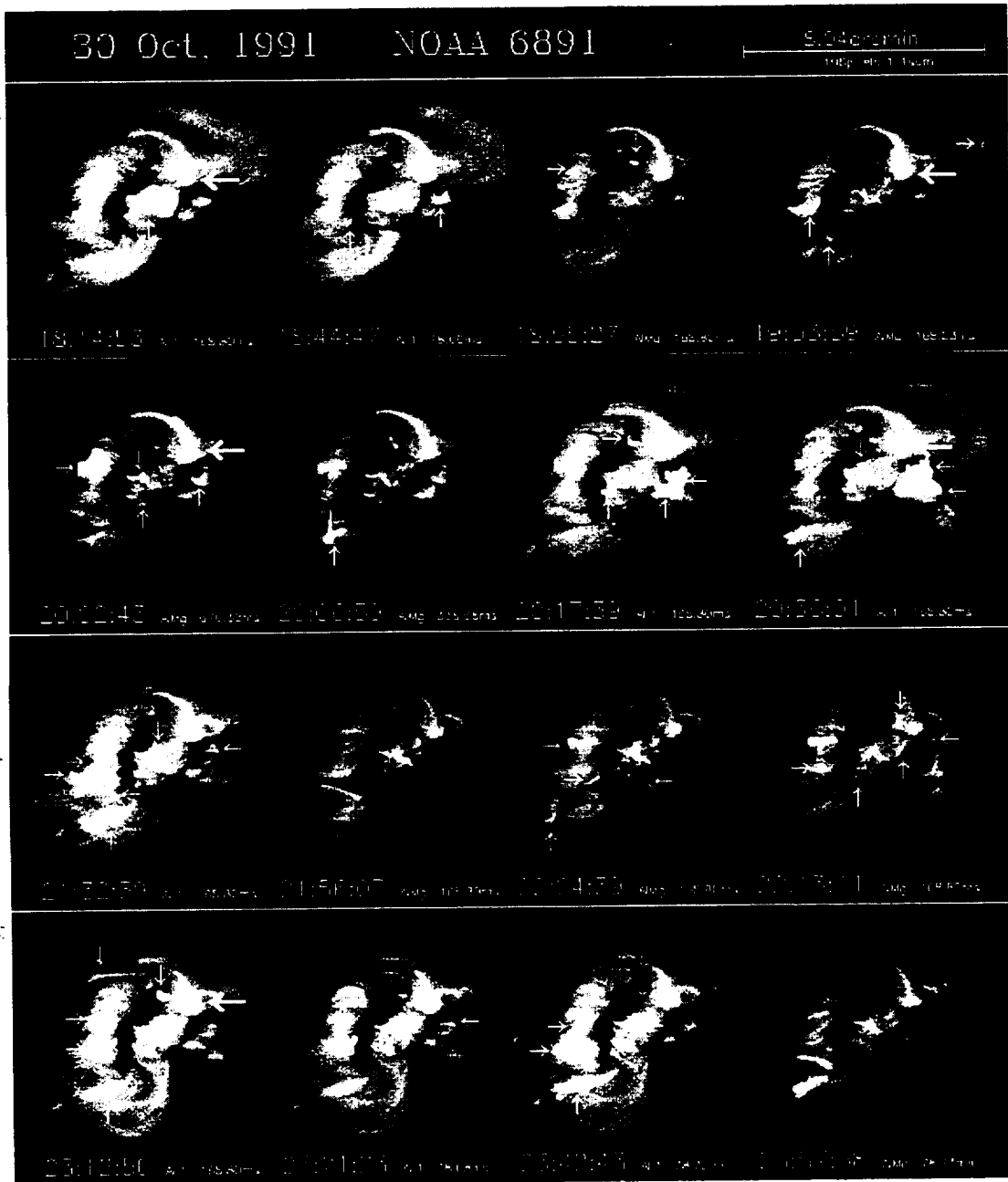


Fig. 4. A time sequence of x-ray images from *Yohkoh*, showing successive transient brightenings in active region loops.

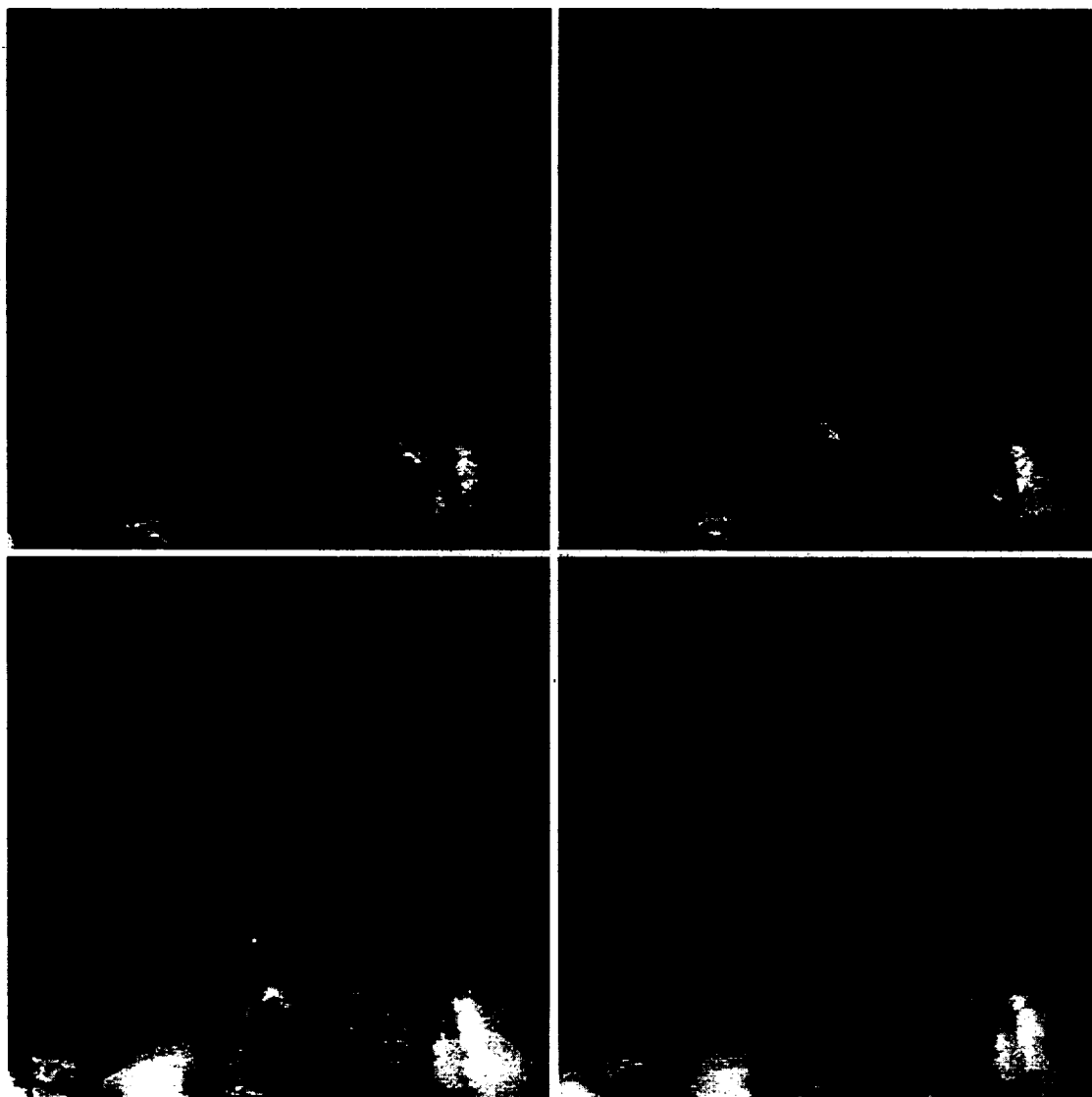


Fig. 5. The 'scorpion' flare, a large filament eruption event observed by the *Yohkoh* SXT on 26 Feb. 1992.

during the flare decay stage is often invoked.

4. Long-Term & Solar Cycle Variations

The most dramatic difference seen in coronal imaging data between solar minimum and other phases of the solar cycle is the vast increase in the number of x-ray bright points (XBP) seen at minimum (Golub 1980). There is considerable controversy concerning the nature of XBP, i.e. whether they represent new magnetic flux reaching the surface, or reprocessed magnetic

flux from previous active region emergence (see Harvey-Angle 1993 for a thorough review). However, the observational fact is undeniable that at solar minimum the low corona is dominated by these small-scale features.

As an example, Fig. 6 shows a comparison between two x-ray images taken a few years apart. The top image was taken in 1973, during the declining phase of that cycle and the bottom image was taken in 1976, at solar minimum. The data were selected at times when the averaged sunspot numbers were nearly identical, so that the instantaneous level of flux emergence was not a factor. Nevertheless, there is a clear difference between the two observations in the number of small features seen: the solar minimum corona is seen to have triple the number of small-scale features. It even appears that there is very little structure in the corona other than that associated with the XBP.

Finally, the changes in x-ray luminosity and in structural composition of the corona as a function of phase in the magnetic cycle are again shown with dramatic clarity by the *Yohkoh* SXT. Figure 7 shows how the corona has evolved during four years of observations by the SXT. The overall soft x-ray luminosity has decreased by a factor of twenty in that time and the large-scale structure, representing the evolved magnetic field of large active regions, has been replaced by the weaker, less organized field structure of the numerous x-ray bright points.

5. Future Observations

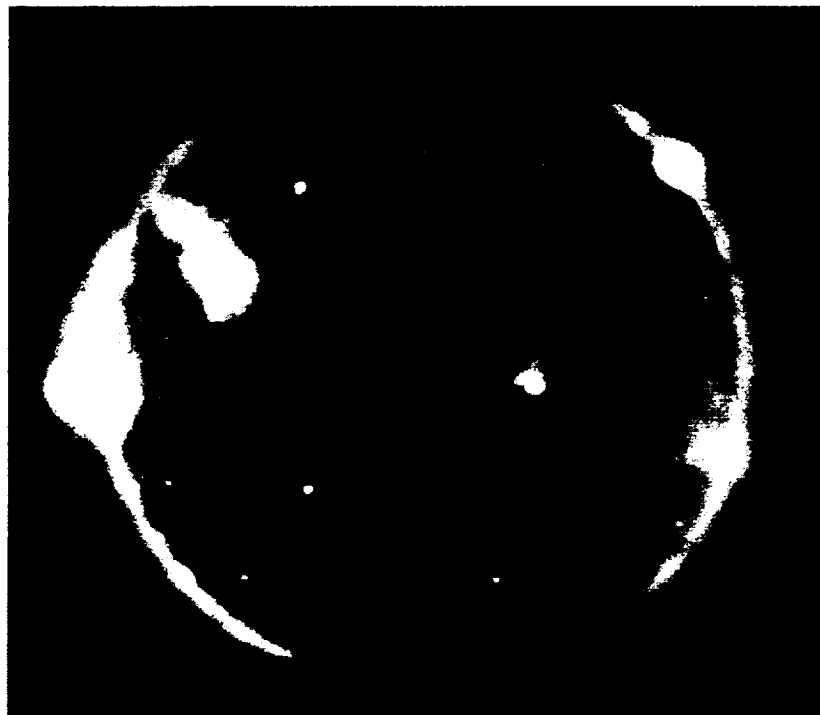
With the launch of the Solar and Heliospheric Observatory (SoHO) by ESA and NASA at the end of 1995, a major new observational capability is added to the solar arsenal. Combined with the *Yohkoh* satellite and with the Transition Region and Coronal Explorer (TRACE) to be launched at the end of 1997, it would appear that solar physics is in a healthy state and that it can look forward to a decade of progress as this millenium closes.

While all of this is true, there are still many areas of solar and solar-terrestrial research which urgently require further attention, both on strictly scientific grounds and because of their direct importance to society. It is now becoming apparent that relatively small changes in the solar output can lead to major changes in the earth's climate, even if the direct cause is not yet clearly understood. Short-term variations, particularly mass ejections and high-speed solar wind streams, are now known to cause damaging effects at ground level, in the upper atmosphere, and in the near-earth space environment. Thus, the activity of the corona has direct consequences for power distribution networks, for the survival of satellites and astronauts in space, for long-range communications, and possibly even for long-term global climate changes.

A wide range of instrumentation will be used in attacking these prob-



16 August 1973



17 November 1976

Fig. 6. Comparison of the XBP number density during the declining phase of the solar cycle (top) and solar minimum (bottom).

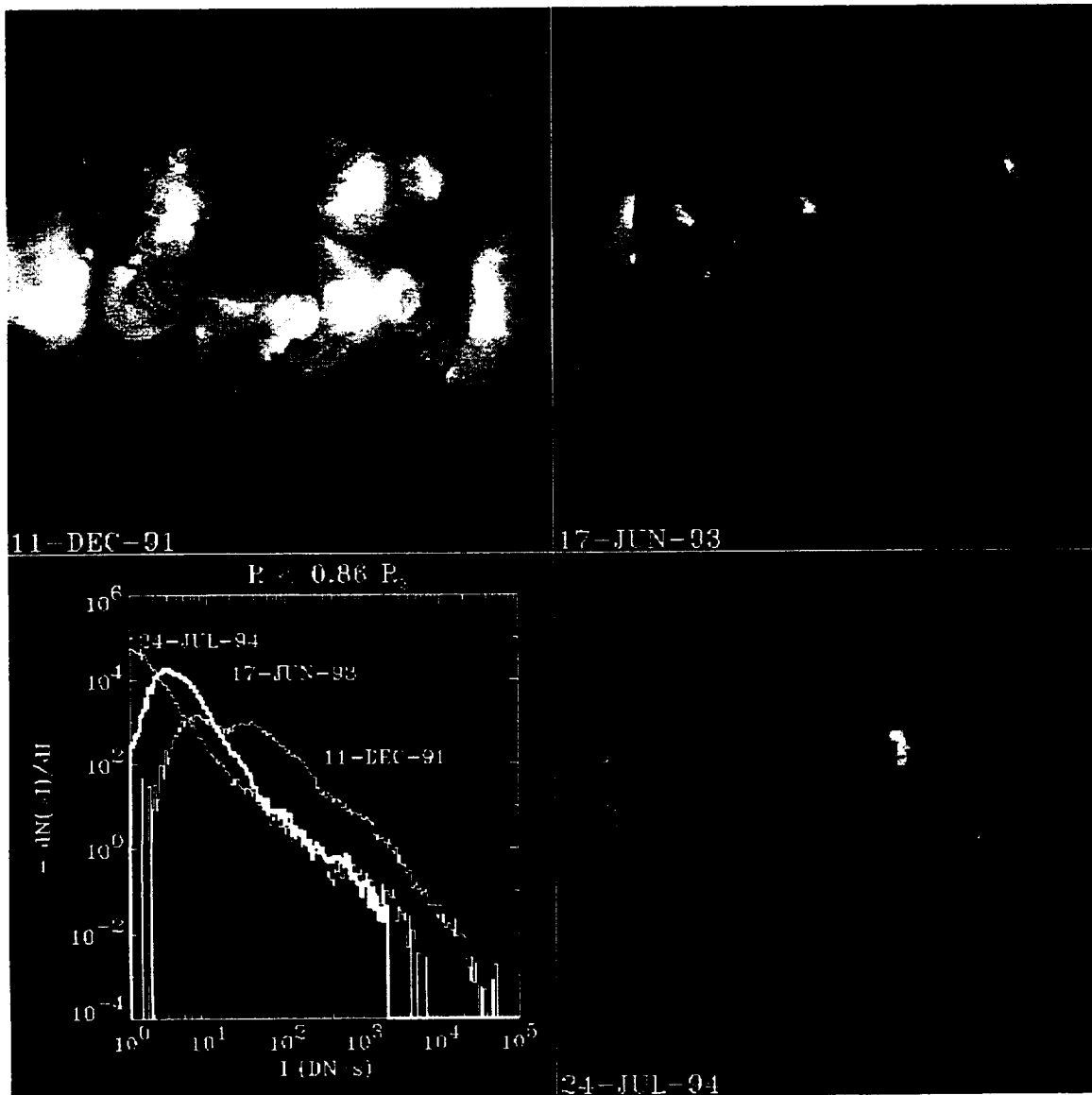


Fig. 7. Change in the coronal x-ray emission as a function of phase in the solar cycle, as seen by the Yohkoh SXT (photo courtesy H. Hara, NAOJ).

lems, including ground-based observing networks, NASA sounding rockets and other rapid, low-cost methods for putting instruments in space, and also larger missions such as the planned Solar-B observatory. A Solar Probe mission would allow direct *in situ* measurements relevant to coronal heating and solar wind acceleration, as well as offering the possibility of obtaining observations of the coronal structure with unprecedented effective spatial

resolution. It is, of course, impossible to predict how much of this will actually happen.

Acknowledgements

I would like to thank Dr. E. DeLuca for helpful discussions and Dr. T. Hartquist for a critical reading of the manuscript. I am also grateful to Drs. L. Acton, H. Hara and T. Shimizu for providing illustrations used in this chapter.

References

- Baum, W.A., Johnson, F.S., Oberly, J.J., Rockwood, C.C., Strain, C.V. and Tousey, R.: 1946, 'Solar Ultraviolet Spectrum to 88 km', *Phys. Rev.* **70**, 781.
- Dunn, R.B.: 1971, 'Coronal Events Observed in 5303Å', in *Physics of the Solar Corona*, ed. C.J. Macris, D. Reidel Publ. Co., Dordrecht-Holland.
- Frazier, E.N. and Stenflo, J.O.: 1972, 'On the Small-Scale Structure of Solar Magnetic Fields', *Sol. Phys.* **27**, 330.
- Golub, L.: 1991, 'X-ray Observations of Global Solar Activity', in *Flare Physics in Solar Activity Maximum 22*, ed. Y. Uchida, *et al.*, Springer-Verlag, Berlin.
- Golub, L.: 1980, 'Solar X-ray Bright Points', *Phil. Trans. Royal Soc. London A* **297**, 595.
- Golub, L., Herant, M., Kalata, K., Lovas, S., Nystrom, G., Pardo, F., Spiller, E. and Wilczynski, J.: 1990, 'Sub-arcsecond Observations of the Solar X-ray Corona', *Nature*, No. 6269, 842.
- Golub, L., Krieger, A.S., Silk, J.K., Timothy, A.F. and Vaiana, G.S.: 1974, 'Solar X-ray Bright Points', *Astrophys. J. (Letters)* **189**, L93.
- Harvey-Angle, K.L.: 1993, 'Magnetic Bipoles on the Sun', Ph.D. Thesis, U. of Utrecht.
- Jones, B.B., Freeman, F.F. and Wilson, R.: 1968, 'XUV and Soft X-ray Spectra of the Sun', *Nature* **219**, 252.
- Linsky, J.L.: 1980, 'Stellar Chromospheres', *Ann. Rev. Astron. & Astrophys.* **18**, 439.
- Linsky, J.L. and Haisch, B.M.: 1979, 'Outer Atmospheres of Cool Stars, I', *Astrophys. J. (Letters)* **229**, L27.
- Narain, U. and Ulmschneider, P.: 1990, 'Chromospheric and Coronal Heating Mechanisms', *Space Sci. Rev.*, **54**, 377.
- Orrall, F.Q. (ed.) 1981. *Solar Active Regions*, Colorado Assoc. Univ. Press, Boulder, Col.
- Robinson, R.D., Worden, S.P. and Harvey, J.W.: 1980, 'Observations of Magnetic Fields on Two Late-Type Dwarf Stars', *Astrophys. J. Lett.* **23**, L155.
- Sheeley, N.R., Jr. and Golub, L.: 1979, 'Rapid Changes in the Fine Structure of a Coronal Bright Point and a Small Coronal Active Region', *Sol. Phys.* **63**, 119.
- Shimizu, T., Tsuneta, S., Acton, L.W., Lemen, J.R., and Uchida, Y.: 1992, 'Transient Brightenings in Soft X-rays Observed by the Soft X-ray Telescope on Yohkoh', *Publ. Astronom. Soc. Japan*, **44**, L147.
- Shimizu, T.: 1994, 'Active Region Transient Brightenings', in *X-ray Solar Physics from Yohkoh*, eds. Y. Uchida, T. Watanabe, K. Shibata and H.S. Hudson, Universal Academy Press, Tokyo, Japan.
- Tandberg-Hanssen, E. and Emslie, A.G. 1988. *The Physics of Solar FLares*, Cambridge University Press UK.
- Vaiana, G.S., Krieger, A.S. and Timothy, A.F.: 1973, 'Identification and Analysis of Structures in the Corona', *Sol. Phys.* **32**, 81.
- Vaiana, G.S., *et al.*: 1981, 'Results from an Extensive EINSTEIN Stellar Survey', *Astrophys. J.* **245**, 163.

- Vaiana, G.S. and Rosner, R.: (1978), 'Recent Advances in Coronal Physics', *Ann. Rev. Astron. Astrophys.* **16**, 393.
- Vaughan, A.H.: 1980, 'Comparison of Activity Cycles in Old and Young Main-Sequence Stars', *Publ. Astron. Soc. Pac.* **92**, 392.
- Wilson, O.C.: 1963, 'A Probable Correlation Between Chromospheric Activity and Age in Main-Sequence Stars', *Astrophys. J.* **138**, 832.
- Wilson, R.: 1964, 'The Zeta/Solar lines Between 170 Å and 220 Å; IAU Symp. No. 23, Liege, Belgium', ed. J-L Steinberg.

Difficulties in Observing Coronal Structure

L. Golub

Smithsonian Astrophysical Observatory
60 Garden St., Cambridge Ma 02138

Abstract

There has developed in recent years a substantial body of evidence to indicate that the temperature and density structure of the corona are far more complicated than had previously been thought. We review some of the evidence and discuss some specific examples: observations of a limb flare, showing that the cool $H\alpha$ material is *cospatial* with the hot x-ray emitting material; simultaneous NIXT and Yohkoh SXT observations of an active region, showing that loops seen in one instrument are not seen in the other, and that the effect works in *both* directions; comparisons of extrapolated magnetic field measurements to the observed coronal structure, indicating that neither potential nor constant- α force-free fits are adequate. We conclude with a description of two new instruments, the TRACE and the TXI, which will help to resolve some of these difficulties.

1 Overview

The importance of magnetic fields in determining the structure of the solar outer atmosphere has long been recognized. Billings (1966) [3] notes that magnetic fields "are employed, as a matter of fact, to explain all departures from a nonspherical [sic] distribution of matter in the corona, including the loop structure of the corona over active regions ...". Observations from sounding rockets in the late 60s and early 70s provided convincing evidence that loops structures, apparently outlining the magnetic field direction, are fundamental (Vaiana, Krieger & Timothy 1973) [28] and the *Skylab* observations in 1973-74 provided the impetus for constructing atmosphere models in which loop "mini-atmospheres" are the fundamental constituent of the inner corona (Rosner, Tucker & Vaiana 1978; Craig, McClymont & Underwood 1978) [18, 7].

This atmosphere is dynamic and constantly varying. Low (1990) [14] notes that the solar atmosphere is never truly quiescent or static, but adds that for the purpose of building models idealized static states may be used as an approximation to the physics underlying the apparent stability of long-lived structures. The extremely dynamic nature of the corona has been shown most effectively by the Soft X-ray Telescope (SXT) aboard the *Yohkoh* satellite: repeated transient loop brightenings in active regions (Shimizu *et al.* 1992) [23], continual rapid expansion outward of structures at the tops of active regions (Uchida *et al.* 1992) [26], jets of x-ray emission, apparently associated with reconnection events (Shibata *et al.* 1992) [22], among others.

Thus, it is already clear that the simplest models of the corona – spherical or plane-parallel – are of limited applicability for interpreting the actual observations, and that the simplest loop atmosphere models – static loops – are also of limited usefulness. To these complications, we will add an additional set of worries, by showing that it is not at all clear that we are even now in a position to say that we know what coronal loops look like, or to know how the real corona is constructed of such loops.

2 Case Studies

In order to illustrate the difficulties alluded to in the Overview, we will examine five specific “case studies”, each involving a seemingly reasonable question about the corona. The questions addressed by these studies are listed in Table 1, along with the answer to each question. The latter will be explained in the course of discussing each case. These examples are all taken from work related to flights of the Normal Incidence X-ray Telescope (NIXT) sounding rocket payload (Golub *et al.* 1990) [6] during the years 1989–1993.

Table 1: Observational questions about the solar corona.

| | |
|--|---|
| Q1. Is the corona hot or cold at a given point in space? | A1. Depends on the viewing method. |
| Q2. Where is the “base” of the corona? | A2. Meaningful only for individual loops and probably unanswerable. |
| Q3. What is the transverse scale size of coronal structures? | A3. Our knowledge is limited by present instrumental resolutions. |
| Q4. What is the relation between the coronal B and x-ray emission? | A4. Data do not provide sufficient constraints. |
| Q5. What does the hot corona look like? | A5. Depends on the viewing method. |

2.1 A limb flare

On 11 Sept. 1989, the NIXT rocket was launched at the start of a small flare (GOES classification C5). However, during the five-minute flight, a second flare began in an active region at the limb (Herant *et al.* 1991) [10]. Examination of the GOES x-ray light curves (Fig. 1) indicates that the limb flare began at about 16:36 UT during the decay phase of the larger on-disk flare. The NIXT observations also began at 16:36 UT, with the last image taken at 16:41:35 UT; the peak of the limb flare in x-rays is at $\approx 16:42$ UT. Thus, the NIXT coverage could not have been better-timed.

Figure 2 shows simultaneous $H\alpha$ and x-ray images of the flare at the time of the peak. The most striking aspect of this event seems to be the nearly identical size, shape and location of flare in the two wavelength regimes. This similarity is confirmed by a cross-correlation between the two datasets, shown in Fig. 3. The

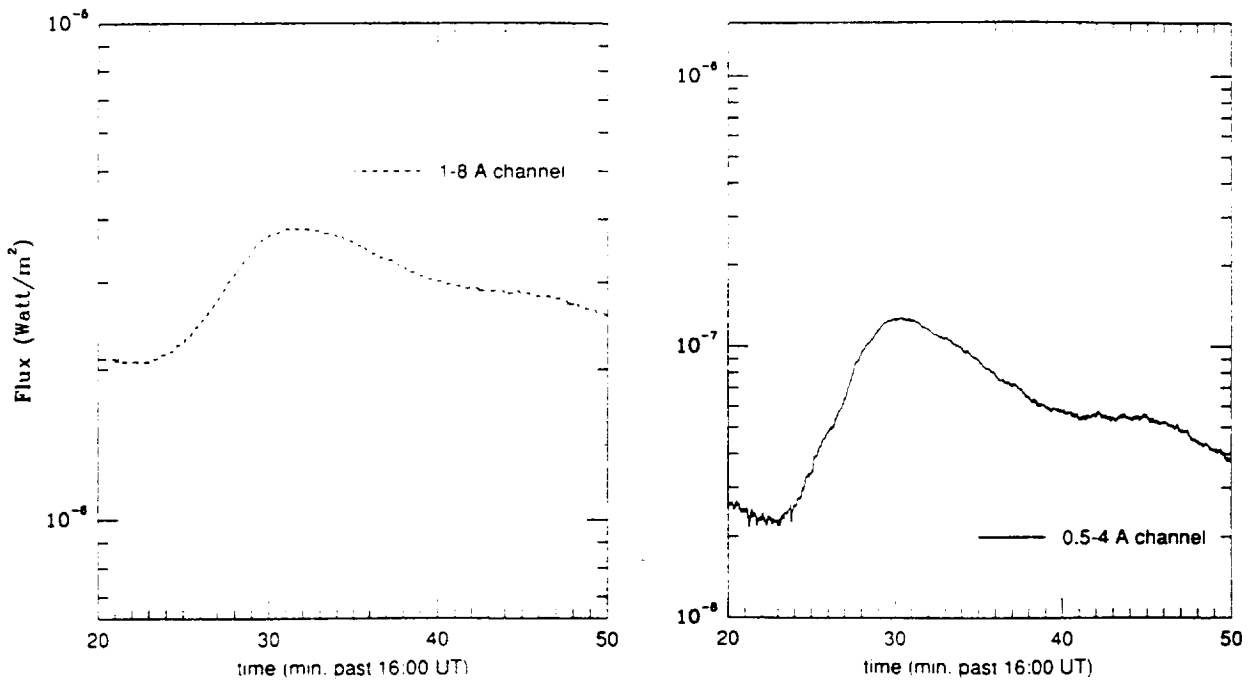


Figure 1: GOES 1-8 Å and 0.5-4 Å x-ray plots for 9/11/89.

contour lines show the x-ray brightness and the shaded region shows the $H\alpha$ brightness: the two overlap to within the accuracy of alignment. Thus it would appear that the corona is both hot (x-ray) and cool ($H\alpha$) at the same place at the same time.



Figure 2: Simultaneous $H\alpha$ and NIXT x-ray images of a limb flare.

Possible explanations exist, of course, for this apparent contradiction. It is possible that the x-ray emission originates from a thin shell ahead of the advancing $H\alpha$ region. Alternatively, hot and cool material may be intermingled on small spatial scales within the observed regions. The problem is not to come up with an answer, it is to come up with a *correct* answer.

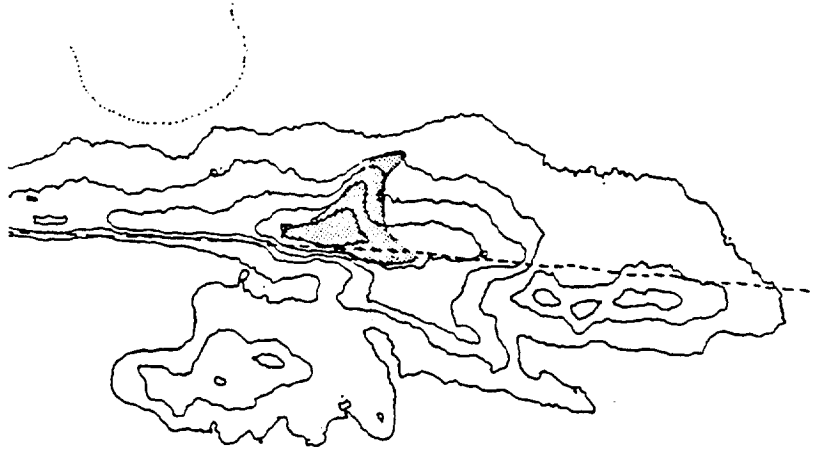


Figure 3: Relative positions of x-ray event and H α material.

2.2 Simultaneous white light and x-ray imaging

Plane-parallel, or spherically symmetric models of the outer solar atmosphere treat the relation between temperature and height as one-dimensional, although not monotonic since the temperature at first increases with height but then decreases again. With the advent of loop model atmospheres, as described above, this fundamental view did not change in essence, but the temperature vs. height relation is transplanted into each loop instead of into the atmosphere as a whole. However, a flight of the NIXT payload on 22 February 1991 provided a unique dataset which shows that a more complicated geometry is required in order to explain the observations.

The multilayer mirrors used in the NIXT to provide x-ray imaging also reflect visible light with $\approx 50\%$ reflectivity. In order to record only the (much fainter) x-ray image, two stages of visible-light rejection are employed: an entrance aperture filter, which cuts the visible to $\approx 1\%$ and a focal plane filter, which provides 10^9 reduction in the visible. During the launch phase of the Feb. '91 flight, a portion of the entrance aperture filter broke. The instrument, however, was designed so that the focal plane filter acts as a back-up in the event of just such a failure. Thus, because the x-rays and the visible are reflected in the same way from the same mirror at the same time, we obtained simultaneous images of the visible disk and the corona. These are automatically coaligned and have the same plate scale, so that high precision ($< \text{one arcsecond}$) comparison between the two can be made.

Figure 4 shows a portion of the east limb from one of the exposures obtained on that flight. Note that there is a dark band at the limb, between the white light solar limb and the bright coronal x-ray emission. We note several features of this gap: 1.) it is most clearly evident when there is an x-ray emitting region behind the limb and no emitting region in front of the limb; 2.) the thickness of the gap varies between equator and poles, or between active regions and large scale "quiet" regions; 3.) at both the inner (white light) and outer (x-ray) heights, the gap is quite sharp. The question we will address is, how is this gap to be interpreted?



Figure 4: Portion of a combined NINT/White Light image, showing a gap between the visible limb and the "base" of the corona, 22 Feb. 1991.

The data from this flight have been analyzed by Daw *et al.* (1995) [4], who find that a model in which the corona is viewed as consisting of a homogeneous set of loops, with temperature varying as a function of height in a uniform manner (Fig 5a) is not consistent with the data. In order to explain what is seen, it is necessary to use a model in which hot loops penetrate downward into an atmosphere having cool spicular material penetrating upward (Fig 5b). The two types of loops do not connect physically, but are interspersed along the line of sight. Thus, the gap is interpreted as the upward extent of spicular material, viewed along the line of sight at the limb and absorbing the x-rays emanating from loops *behind* the spicules.

We note that the soft x-rays in the NINT data are strongly absorbed in spicular material, with about 10 arcsec path length required for $1/e$ absorption. The variation in thickness of the band indicates that spicules may extend farther in open field (e.g. coronal hole) regions than in higher temperature closed-loop regions, as reported by Huber *et al.* (1974) [12]. This interpretation of the NINT data suggests that the footpoints of coronal loops cannot, in principle, be seen. When viewed at the limb, they are obscured by the intervening spicule material; when viewed from above, the projection angle is such that the height of the coronal "base" is very poorly determined. Depending upon the relative spatial density of hot vs. cool structures, there may be a small range of locations near the center of the disk which allow for both viewing the loops at an angle and for viewing them unobstructed. However, this is not yet known.

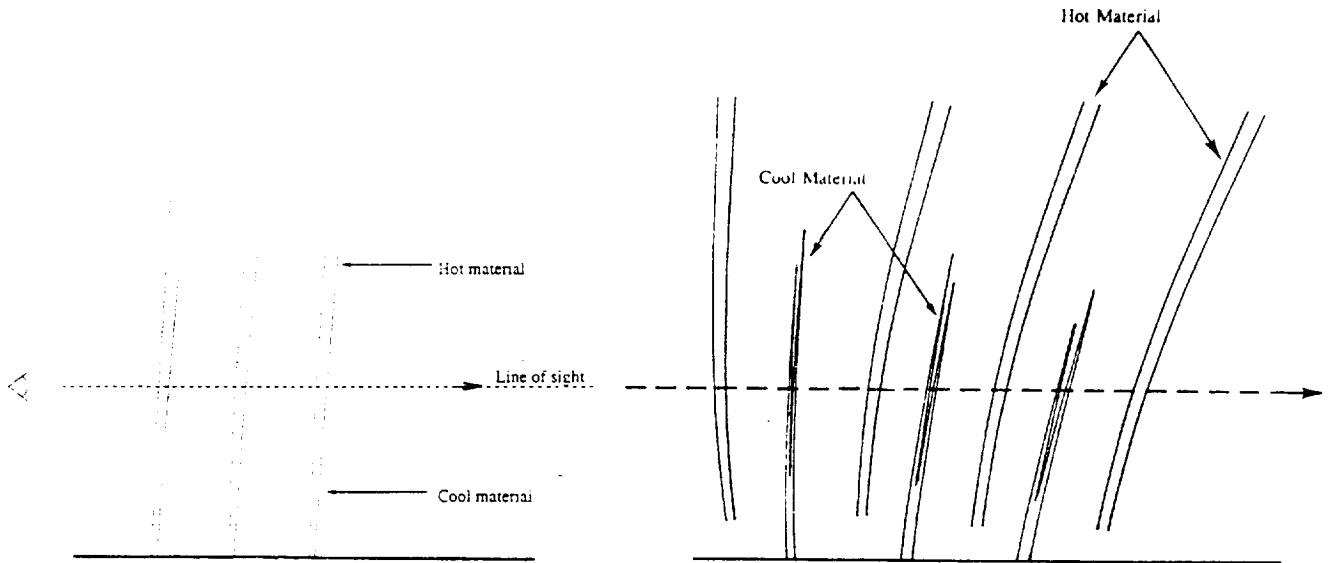


Figure 5: Two loop model atmospheres offering alternative explanations of the gap seen in Fig. 4. Modified plane-parallel model on left does not fit the data.

2.3 Active region fine structure

The progress in x-ray optics, when applied to solar coronal imaging, has consistently revealed coronal fine structure down to the resolution limit of the observing instruments (see, e.g. articles by Giacconi, Golub and Walker *et al.* in Linsky & Serio, 1993 [13]). An example is shown in Fig. 6, a coronal x-ray image from the NIXT instrument, obtained on 11 July 1991. There is clearly fine structure prevalent everywhere in the image and photographic analysis indicates that it reaches the combined limit set by the film and by the pointing stability of the rocket.

A quantitative analysis of the fine structure of several active regions observed by the NIXT was carried out by Gómez *et al.* (1993) [9]. By Fourier analyzing the images, they find a broad, isotropic power-law spectrum for the spatial distribution of soft x-ray intensities. The spectrum has a slope of $\alpha \approx -3$, which extends down to the resolution limit of the instrument at ≈ 0.75 arcsec.

A similar result has been obtained by Martens & Gómez (1992) [15] from analysis of *Yohkoh* SXT data: the Fourier transform distribution is a power-law (with somewhat smaller slope of $\alpha \approx -2.4$) which extends down to the Nyquist frequency. Thus, for both cases in which the procedure has been carried out, the spatial structuring of the corona is seen to be limited by the resolution of the imaging instrument. The implication, since the sun does not know what instrument we are using to observe it, is that we have not yet fully resolved the coronal fine structure. Thus, the answer to Question 3, "What is the transverse scale size of coronal structures?", is that we do not yet know.



Figure 6: 11 July 1991 NIXT image.

2.4 Magnetic field extrapolation vs. observed structure

There have been only a limited number of attempts in recent years to carry out direct comparisons between high resolution coronal observations and magnetic field extrapolations, if we exclude attempts to explain the onset of flares by testing the non-potentiality of fields. For non-flaring regions, i.e. normal coronal structure, Poletto *et al.* (1975) [17] and Sakurai & Uchida (1977) [19] had reasonable success at the level of late 60s and early 70s resolution. More recently Sains *et al.* (1992) [20] found a general agreement between extrapolations and the structures seen in the NIXT, although close examination shows that the agreement is quite poor in detail. Metcalf *et al.* (1994) [16] conclude, from comparison of vector magnetograph data (giving the locations of vertical currents) with Yohkoh SXT coronal data, that there is a very poor spatial and temporal correlation between the locations of the currents and the locations of bright coronal structures.

In a recent study, Schmieder *et al.* (1996) [21] have used high resolution NIXT data combined with Kitt Peak magnetogram and Multi-channel Double Pass (MSDP) spectrograph data, to study in more detail the relationship between the observed structure and the type of magnetic field extrapolation employed. The extrapolation code is based on the work of Alissandrakis (1981) [1] as modified by Démoulin *et al.* (1996) [5]. A single active region, AR 6718 on 11 July 1991, was chosen for study: an x-ray image of the region and the corresponding portion of the magnetogram are shown in Fig. 7.

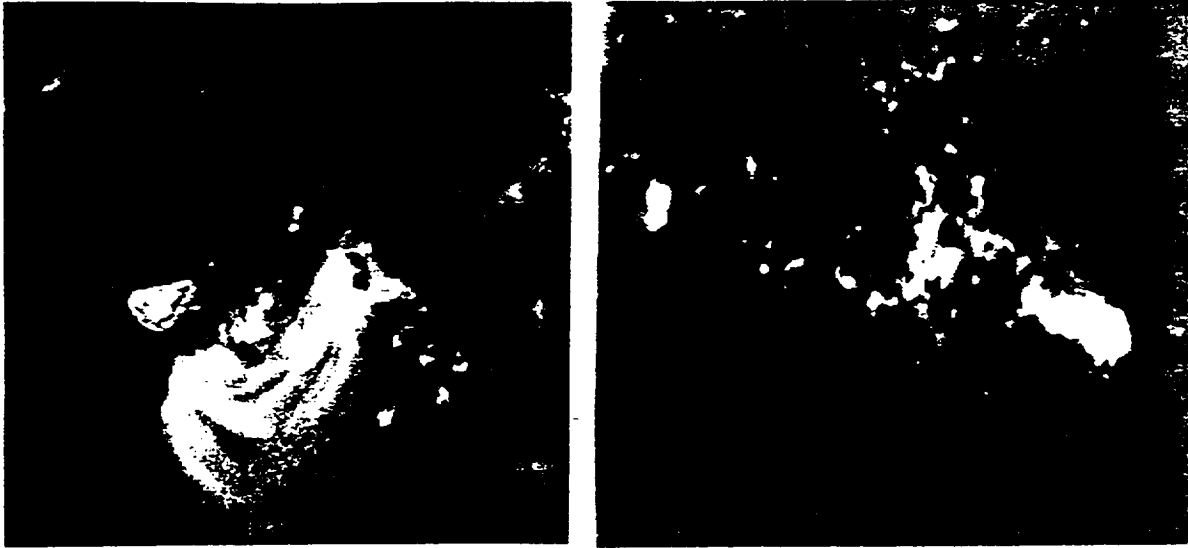


Figure 7: NIXT x-ray image of AR 6718 and KPNO magnetogram of the region.

The first result is that a potential-field extrapolation does not represent the observed coronal structure at all, and that even a constant- α force-free field extrapolation is not adequate. Fig. 8 shows extrapolations using three values of α . The left-most panel shows $\alpha = 0$, i.e. a potential field. Note that the connectivity of the field lines is entirely different from that of the observed structures. The two force-free fits in the middle and right-hand panels match portion of the region, but neither one in itself is a good fit. What we find is that the inner portion of the active region is well matched by the larger value of α while the outer portion of the region is matched by a lower α .

A possible interpretation of this result is that there is, with time, a relaxation of the magnetic field, as proposed by Heyvaerts & Priest (1984) [11]. In a highly-conducting plasma, small-scale processes dissipate magnetic energy much more rapidly than helicity $H \equiv \int \mathbf{A} \cdot \mathbf{B} dV$ (Taylor, 1974; Berger, 1985) [25, 2]. With this constraint the magnetic field does not relax to a potential state, but to a linear force-free state. The gradient of α found in this region may be indicative of this ongoing relaxation process.

2.5 Yohkoh SXT vs. NIXT comparison

In April 1993 the Yohkoh SXT carried out a special observing sequence simultaneous with a flight of the NIXT rocket. An initial comparison of the two datasets was carried out by Yoshida *et al.* (1995) [27] for a quiet corona region. Because the SXT temperature response is somewhat harder than that of the NIXT (> 2.5 MK for SXT vs. $1 - 3$ MK for NIXT) it was expected that the SXT would see the hotter top portions of coronal loops while the NIXT would see the lower portions or the footpoints. This was indeed generally seen to be the case in that study.

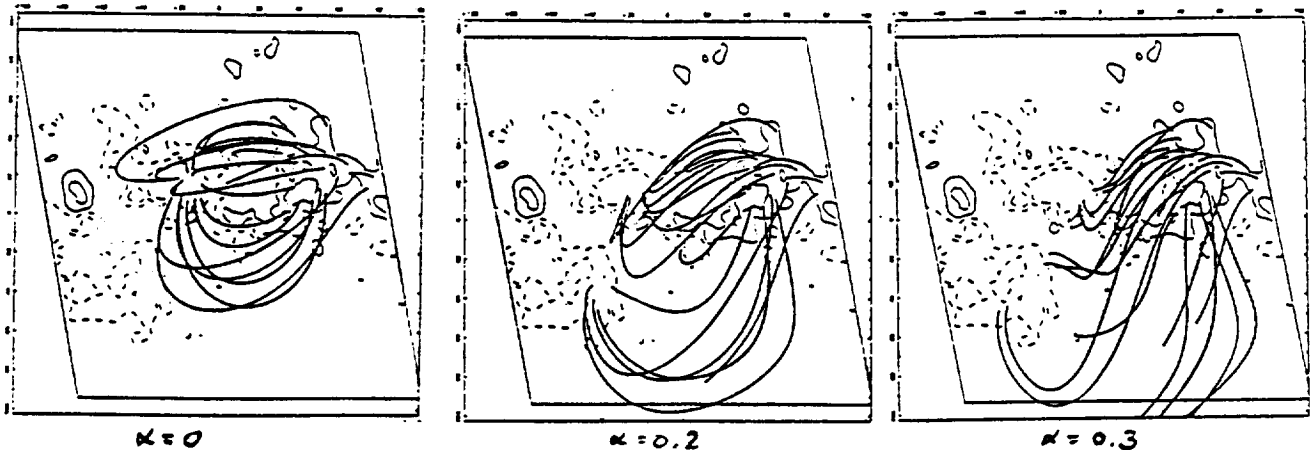


Figure 8: Magnetic field extrapolations of AR 6718. with three values of α .

However, subsequent evaluation of the one active region on the disk on that day is showing a completely different and unexpected result. One expects that “all x-ray images are alike”, so that the two should show roughly similar structures. Viewed from a distance, the two observations seem to be showing the same coronal features. However, detailed examination shows some remarkable discrepancies between the two.

Fig. 9 shows the comparison of NIXT and Yohkoh SXT observations, with arrows pointing to three locations in the region. These are places where a structure or set of structures is visible in one of the images and *entirely invisible* in the other; the effect works both ways. Thus, if only one of these images were available, we would draw erroneous conclusions about the coronal structure, since there would be no indication at all that some structures are present.

The seriousness of this problem is obvious: if we intend to study the formation, stability and dynamics of coronal structures, one must first be able to see them. A partial solution to this problem is described in the next section.

3 Some Partial Solutions

The above discussion provides only a partial listing of some of the problems we are encountering in attempting to study the formation, heating, structuring and dynamics of the solar corona. In this section we describe two new instruments which will help to solve, or at least advance, some of these problem areas. The TRACE instrument will have the highest spatial resolution ever used to observe the corona, as well as the ability to discriminate multiple temperature regimes and to view the atmosphere from the upper chromosphere up into the active region corona. The TXI is a rocket-borne payload which will have the capability of observing the entire sequence of successive ionization stages of a single element from $< 10^6$ K to $> 3 \times 10^6$ K, and will also determine flow velocities at these temperatures.

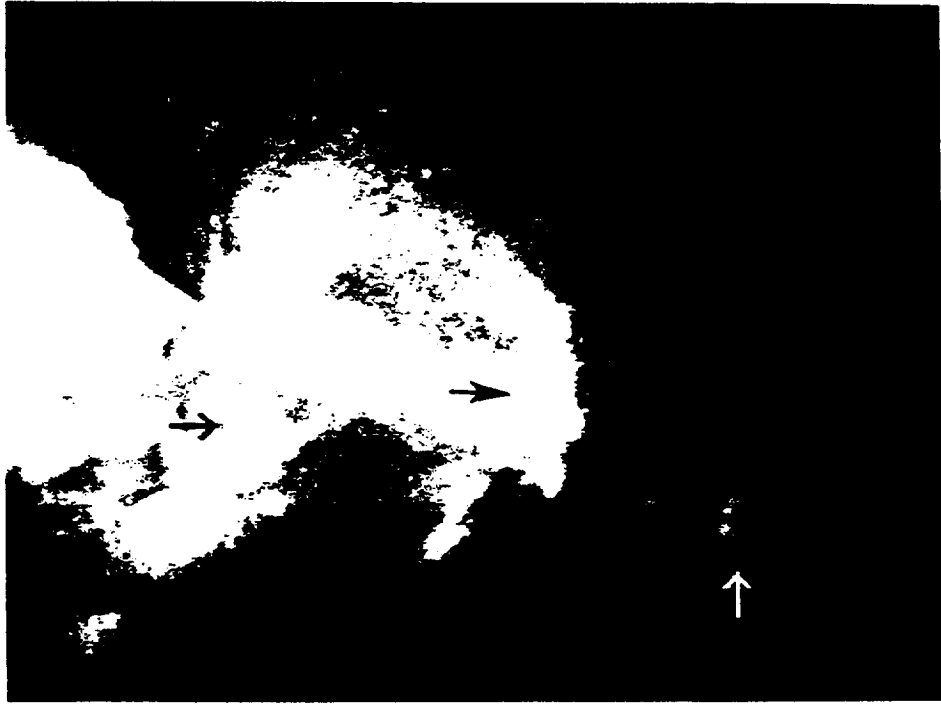
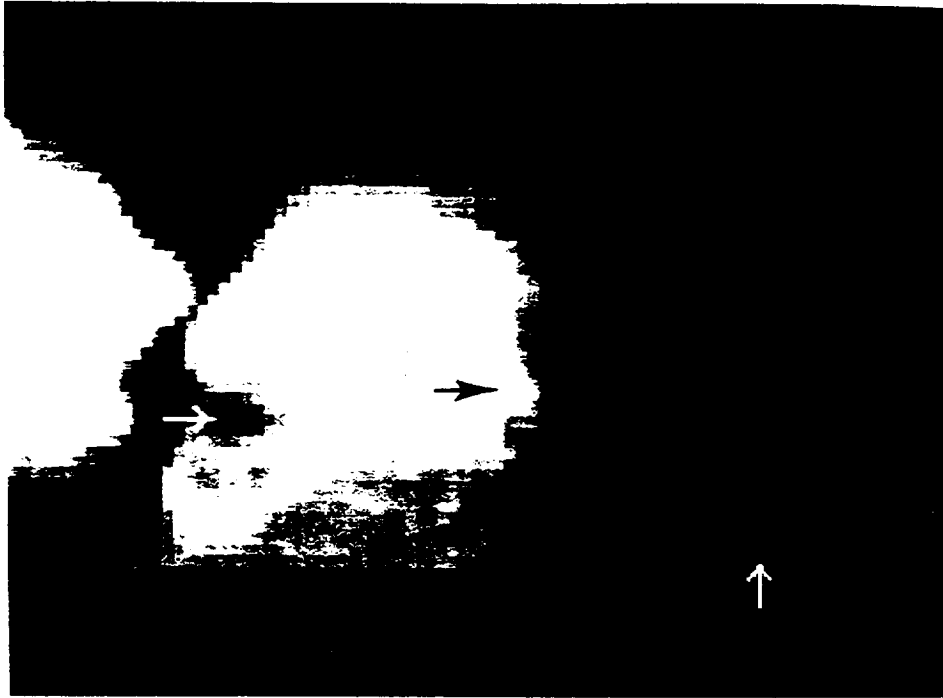


Figure 9: Comparison between Yohkoh SXT (top) and NIXT (bottom) observations of an active region: arrows indicate structures seen in one of the instruments but *not* seen in the other.

Table 2: TRACE spectral regions & observing parameters.

| Central Wavelength (\AA) | Width (\AA) | Ion | Location |
|-------------------------------------|------------------------|-------------------|-------------------|
| 2500 | Broad | Continuum | Photosphere |
| 1700 | " | T_{min} /Chrom. | |
| 1570 | 30 | C I, Fe II, Cont. | " |
| 1550 | 30 | C IV | Transition Region |
| 1216 | 84 | H Ly α | Chromosphere |
| 284 | 14 | Fe XV | Corona |
| 195 | 10 | Fe XII | " |
| | | (+Fe XXIV) | Flares |
| 171 | 9 | Fe IX | Corona |

3.1 TRACE

The Transition Region And Coronal Explorer (TRACE) is designed to quantitatively explore the connections between fine-scale magnetic fields at the solar surface and the associated plasma structures in the solar outer atmosphere. The TRACE instrument uses multiple UV and normal-incidence XUV channels to collect images of atmospheric plasma from 10^4 K to 10^7 K. Many of the physical problems that arise in this portion of the atmosphere – plasma confinement, reconnection, wave propagation, plasma heating – arise throughout space physics and much of astrophysics as well. Although recent progress in, e.g., numerical MHD simulations has been substantial (*viz.* Low 1990), use of these models requires close guidance by the observations, because the enormous range in parameter scale sizes cannot be realized in the computations.

The telescope provides true one arcsecond resolution (1 pixel is 0.5 arcsec) and temporal resolution as short as a fraction of a second for bright sources. Table 2 lists the operating spectral bands, the associated temperatures and the portions of the atmosphere covered. The instrument uses four normal incidence coatings, one for broadband UV and three for narrowband XUV operation. The UV channel includes a set of narrowband filters at the focal plane, thereby allowing sub-channels which detect portions of the atmosphere from the photosphere to the transition region. Selection of the XUV channels is based on a thorough analysis carried out by Golub, Hartquist & Quillen (1989), who analyzed the spectral region accessible to normal incidence techniques and determined the best lines to use for particular atmospheric features of interest.

TRACE is launched on a Pegasus-XL into a polar, sun-synchronous orbit, thereby providing continuous observation of the sun. Continuous observing for about 8 months is planned over a 1-year baseline mission. TRACE produces data complementary with SOHO, and planning of the TRACE daily observations is being coordinated with those of SOHO.

The main components of the TRACE instrument are shown in Fig. 10. The TRACE instrument consists of a 30 cm diameter Cassegrain telescope and a fil-

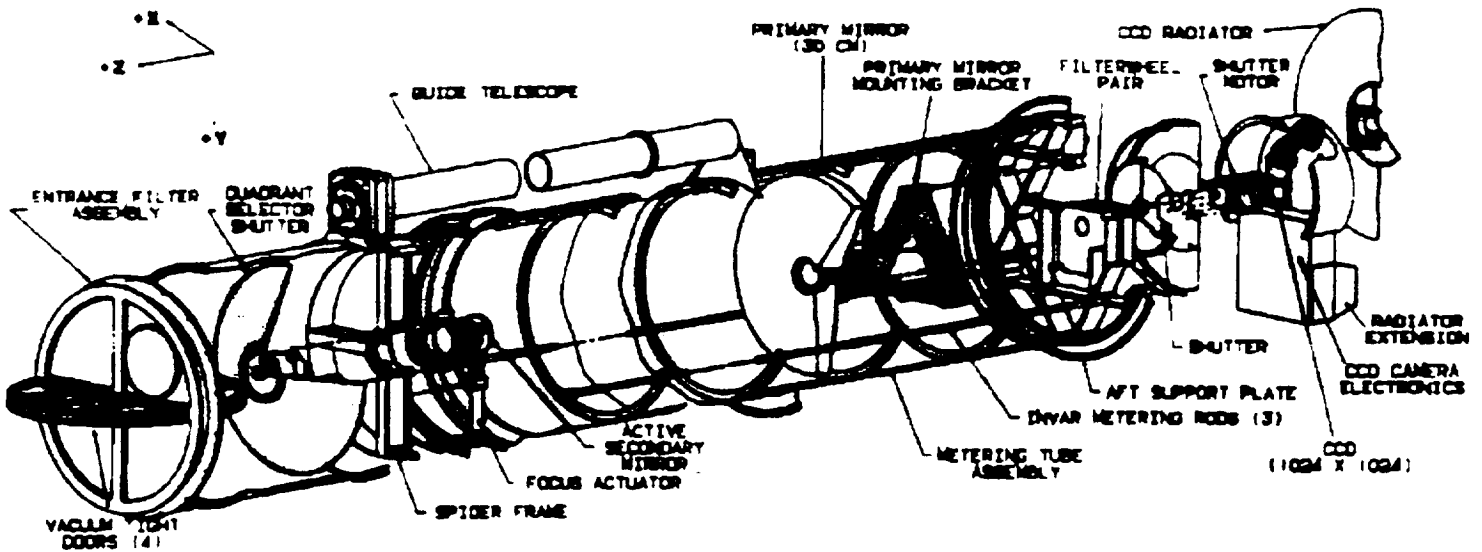


Figure 10: Major system components of the TRACE instrument.

ter system feeding a CCD detector. Each quadrant of the telescope is coated for sensitivity to a different wavelength range. Light entering the instrument passes first through an entrance filter assembly which transmits only UV and soft x-ray radiation, thus blocking the solar heat from reaching the mirrors. A large rotating quadrant shutter selects one quadrant at a time for viewing. The secondary mirror of the telescope is active, to correct for pointing jitter to better than 0.1 arcsec.

The converging beam from the secondary mirror passes through the central hole in the primary, where it encounters two filter wheels in series, each having three filters and one open position. These wheels contain both the XUV light-blocking and the UV passband filters. Finally, there is a focal plane shutter and a 1024X1024 CCD, for a field of view of 8.5X8.5 arcmin. Mosaic observations are planned, for larger field and daily full disk data-taking. The TRACE launch is late in 1997, and mission lifetime is at least 8 months. Thus it will be observing during the rise phase of the new solar cycle.

Some of the scientific objectives of the mission are:

- Magnetic Field Structure and Evolution.
- Coronal Heating and Magnetic Fields.
- Onset of Coronal Mass Ejections.
- Variability of X-ray Bright Points.

The mission and its objectives are described in more detail in Tarbell *et al.* (1994).

3.2 TXI

The Tuneable X-ray Imager (TXI) is a high resolution coronal imaging instrument which has the ability to produce near-monochromatic images tuneable over a range of XUV wavelengths. The present design covers the wavelength range 170 - 220 Å, which includes the strong series of iron lines from Fe IX through Fe XIV, inclu-

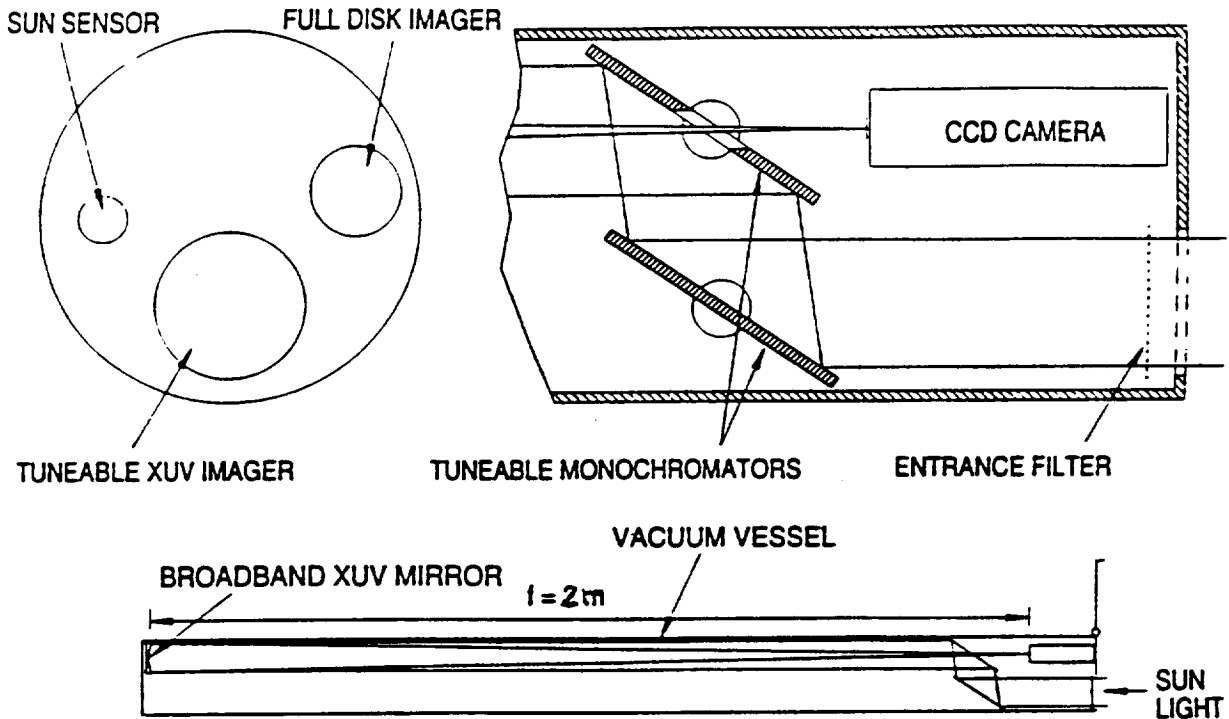


Figure 11: Schematic layout of the Tuneable XUV Imager.

sive. Thus, the problem of “missing” structures is solved, for the temperature range $\log T = 5.8 - 6.4$, because *all* of the successive ionization stages are isolated and recorded.

Figure 11 shows a schematic layout of the instrument. Spectral isolation is achieved by using a double-crystal monochromator, which feeds a broadband telescope, coated with an XUV multilayer having $\Delta\lambda \sim 30 \text{ \AA}$ (FWHM). The monochromator is made as narrowband as possible, which in this instance is $\approx 4 \text{ \AA}$, and it is tuned by rotating the two plane mirrors in parallel. A Cowan-Golovchenko arrangement is used (Cowan 1983), which has the highly desirable property that the entrance and exits beams stay fixed during tuning. Thus, there is no image motion in the focal plane as the wavelength is changed.

Table 3.2 shows the strongest lines in the TXI passband. Depending upon line strength and available exposure time, it appears possible to record data out to $\approx 220 \text{ \AA}$; no data below 170 \AA are recorded because aluminum light-blocking filters are used at the entrance aperture and at the focal plane. We note that line multiplets, such as Fe XII near 193 \AA , do not smear the image, because this is a non-dispersive system.

The TXI sounding rocket program has just received approval from NASA to begin construction (May 1996). Present plans are to have the payload ready to fly in two years, by the summer of 1998. A summer launch is necessary in order to reduce absorption by the residual even at rocket altitudes. A minimum altitude of 100 miles is necessary for the wavelengths observed in this experiment, and a line-of-sight to the sun as near normal to the plane of the atmosphere as possible is required. The launch therefore takes place around local noon in White Sands, NM.

Table 1. Strongest lines in the TXI passband.

| Ion | Wavelength (\AA) | $\log T$ |
|--------------|-----------------------------|----------|
| Fe IX | 171.08 | 6.0 |
| O V | 172.17 | 5.4 |
| O VI | 172.94 | 5.5 |
| | 173.08 | |
| Fe X | 174.53 | 6.1 |
| | 177.24 | |
| Fe XI | 180.42 | 6.2 |
| Si XI/Fe XII | 186.88 | 6.2 |
| Fe XI | 188.22 | 6.2 |
| Fe XXIV | 192.03 | 7.3 |
| Fe XII | 192.40 | 6.2 |
| | 193.52 | |
| | 195.13 | |
| Fe XIII | 202.04 | 6.2 |
| | 203.82 | |
| Fe XIV | 211.32 | 6.3 |
| He II | 237.35 | 4.7 |

3.3 The Solar Radio Telescope

Of course, it is not only in the area of space-based instrumentation that solutions to the present set of problems in solar physics may be sought. In this section we describe a representative ground-based instrument, designed to map the magnetic field structure and topology in the corona.

A proposal for a dedicated Solar Radio Telescope which represents a major advance on current radio facilities is currently being explored (a report by D. Gary and T. Bastian will be available shortly). The ability to map solar magnetic fields above coronal active regions is one of the major goals of this telescope. The features necessary to carry out such a goal are:

- the ability to make radio images of active regions on short timescales with high spatial resolution and high dynamic range;
- the ability to make images at many closely-spaced frequencies across a broad frequency range nearly simultaneously; and
- accurate polarimetry.

The proposed instrument which provides these features consists of an array which contains many small dishes (presently planned to be 40) with full-disk coverage, three large (~ 25 m) dishes to provide sensitivity and allow accurate calibration, and receivers which incorporate the frequency-agile characteristics so successfully demonstrated by the OVRO array with a target range from 300 MHz to 30 GHz. This instrument would have 2.5 times as many baselines as the VLA, and requires a

large correlator to handle them. Recent advances in broadband microwave components, large correlators and computers make such an instrument possible for a low cost. Considerable effort will also be expended on software for real-time processing of the data into a form (images and coronal field maps) suitable for immediate use by the broader solar community.

3.3.1 Vector magnetic fields

Finally, we mention the almost obvious point that vector magnetograms are crucially important in the comparison between surface fields and coronal structure/stability. Ground-based observations have progressed enormously, but there still remains the basic question: how much of the observed variability is due to atmospheric effects and how much is intrinsic to the source? This question has been answered in part by comparing observations taken simultaneously at widely-separated sites. However, the best way to answer the question and to obtain the highest quality observations, is to place a vector magnetograph in orbit.

References

- [1] Alissandrakis, C.E. 1981. *Astron. & Astrophys.* **100**, 197.
- [2] Berger, M.A. 1985. *Astrophys. J. Suppl.* **59**, 433.
- [3] Billings, D.E. 1966. *A Guide to the Solar Corona*, Academic Press, New York.
- [4] Daw, A., DeLuca, E. and Golub, L. 1995. *Astrophys. J.* **453**, 929.
- [5] Démoulin, P., Balalá, L.G., Mandrini, C.H., Hénoux, J.C. and Rovira, M.G. 1996. *Astron. & Astrophys.* (in press).
- [6] Golub, L., Herant, M., Kalata, K., Lovas, S., Nystrom, G., Pardo, F., Spiller, E. and Wilczynski, J. 1990. *Nature*, No. 6269, 842.
- [7] Craig, I.J.D., McClymont, A.N. and Underwood, J.H. 1978. *Astron. & Astrophys.* **70**, 1.
- [8] Golub, L., Hartquist, T.W. and Quillen, A.C. 1989. *Sol. Phys.* **122**, 245.
- [9] Gómez, D.O., Martens, P.C.H. and Golub, L. 1993. *Astrophys. J.*, **405**, 767.
- [10] Herant, M., Pardo, F., Spiller, E. and Golub, L. 1991. *Astrophys. J.* **376**, 797.
- [11] Heyvaerts, J. and Priest, E.R. 1984. *Astrophys. J.* **137**, 63.
- [12] Huber, M.C.E., Foukal, P.V., Noyes, R.W., Reeves, E.M., Schmahl, E.J., Timothy, J.G., Vernazza, J.E. and Withbroe, G.L. 1974. *Astrophys. J. (Letters)* **194**, L115.
- [13] Linsky, J.F. and Serio, S., eds. 1993. *Physics of Solar and Stellar Coronae*, Kluwer Academic Publishers, Dordrecht, Holland.
- [14] Low, B.C. 1990. *Ann. Rev. Astron. Astrophys.* **28**, 491.
- [15] Martens, P.C.H. and Gómez, D.O. 1992. *Publ. Astronom. Soc. Japan*, **44**, L187.
- [16] Metcalf, T.R., Canfield, R.C., Hudson, H.S., Mickey, D.L., Wülser, J.P., Martens, P.C. and Tsuneta, S. 1994. *Astrophys. J.*, **428**, 860.

- [17] Poletto, G., Vaiana, G.S., Zombeck, M.V., Krieger, A.S. and Timothy, A.F. 1975. *Sol. Phys.* **44**, 83.
- [18] Rosner, R., Tucker, W.H. and Vaiana, G.S. 1978. *Astrophys. J.*, **220**, 643.
- [19] Sakurai, T. and Uchida, Y. 1977. *Sol. Phys.* **52**, 397.
- [20] Sams, B.J., III, Golub, L. and Weiss, N.O. 1993. *Astrophys. J.*, **399**, 313.
- [21] Schmieder, B., Démoulin, P., Aulanier, G. and Golub, L. 1996. *Astrophys. J.* (in press).
- [22] Shibata, K., *et al.* 1992. *Publ. Astronom. Soc. Japan*, **44**, L173.
- [23] Shimizu, T., Tsuneta, S., Acton, L.W., Lemen, J.R., and Uchida, Y. 1992. *Publ. Astronom. Soc. Japan*, **44**, L147.
- [24] Tarbell, T.D., Bruner, M., Jurcevich, B., Lemen, J., Strong, K., Title, A., Wolfson, J., Golub, L. and Fisher, R. 1994. Proc. of the 3rd SOHO Workshop, ESA SP-373, Dec. 1994.
- [25] Taylor, J.B. 1974. *Phys. Rev. Lett.* **33**, 1139.
- [26] Uchida, Y., McAllister, A., Strong, K.T., Ogawara, Y., Shimizu, T., Matsumoto, R., and Hudson, H.S. 1992. *Publ. Astronom. Soc. Japan*, **44**, L155.
- [27] Yoshida, T., Tsuneta, S., Golub, L., Strong, K. and Ogawara, Y. 1995. *Publ. Astron. Soc. Japan* **47**, L15.
- [28] Vaiana, G.S., Krieger, A.S. and Timothy, A.F. 1973. *Sol. Phys.* **32**, 81.

